Jul 12th, 11:30 AM - 11:50 AM

# Investigating the Street Canyon Vegetation Effects Using the Moment Method

Viktor Šíp
*Czech Technical University in Prague*, viktor.sip@fs.cvut.cz

Luděk Beneš
*Czech Technical University in Prague*

*International Environmental Modelling and Software Society (iEMSs)*
*8th International Congress on Environmental Modelling and Software*
*Toulouse, France, Sabine Sauvage, José-Miguel Sánchez-Pérez, Andrea Rizzoli (Eds.)*
*http://www.iemss.org/society/index.php/iemss-2016-proceedings*

# Investigating the Street Canyon Vegetation Effects Using the Moment Method

**Viktor Šíp [a,†], Luděk Beneš [a]**

[a] *Faculty of Mechanical Engineering, Czech Technical University in Prague, Czech Republic*
[†] *viktor.sip@fs.cvut.cz*

**Abstract:** In this paper we investigate the effects of the vegetation inside a street canyon. Flow through and around the standalone street canyon is calculated using a CFD solver based on the Reynolds-averaged Navier-Stokes equations. The dispersion of the pollutant is computed using the moment method that models the behaviour of the particle size distribution. Resulting pollutant concentrations for several wind conditions and for configurations without and with the trees are compared to the wind tunnel measurements. Using the deposition velocity model for the moment method, the effect of the dry deposition on the vegetation is then assessed. Three modes of the particle size distribution - the ultrafine, the accumulation, and the coarse mode - are studied. Results show that the the dry deposition has negligible effects on the accumulation and the ultrafine mode, but can locally reduce the mass concentration of the particles in the coarse mode by more than 10%.

***Keywords:*** Street canyon, Urban vegetation, Dry deposition, RANS modelling, Moment method

## 1 INTRODUCTION

A street canyon is an important subunit of the urban flow and air quality models. Its configuration affects the pedestrian wind comfort and the dispersion of the traffic related pollutants. Street canyon vegetation plays a significant role in both of these aspects and is often investigated using wind tunnel as well as numerical studies (see Janhäll, 2015, for a recent overview).

The pollutant dispersion in the street canyon and the effect of vegetation was extensively studied by Gromke et al. through a series of wind tunnel experiments and CFD simulations (Gromke and Ruck, 2007, 2009; Gromke et al., 2008; Buccolieri et al., 2009, 2011), summarized in (Gromke and Ruck, 2012). Investigating various configurations of the tree avenues under different wind conditions, they found that the tree avenues generally reduce the circulation between the pedestrian level and the level above the rooftops, and therefore increase the concentration below the crown layer. With the decreasing crown porosity, an increase of the concentration at the leeward wall and a smaller decrease at the windward wall was observed for the flow perpendicular to the street. The largest changes were observed for the oblique flow (45° relative to the street direction), where the relative increase of the average concentration at the leeward wall was 146%. However, these studies did not consider deposition on the vegetation.

Vranckx et al. (2015) investigated the annual impact of the trees in the model street canyon in the city of Antwerp, Belgium. They considered the deposition on the vegetation, and to model it, they used several values of constant deposition velocity. Taking into account background concentration and emission rates, they found the annual average increase of the concentration to be in range of 1% to 13% for elemental carbon and between 0.2% to 2.6% for $PM_{10}$, depending on the vegetation porosity and the deposition velocity.

Constant deposition velocity does not fully reflect the complex process of the dry deposition on the vegetation. Measurements showed that the deposition velocity is highly dependent on the wind speed, on the particle size and on the vegetation species, with differences on the orders of magnitude (Litschke and Kuttler, 2008; Janhäll, 2015). It is accepted that different processes play significant roles for different particle sizes. The particles larger than 10 µm are most affected by the sedimentation process, while the particles smaller than 0.1 µm deposit mainly due to the Brownian diffusion. In the range in between these values the processes of impaction and interception play the major role. The deposition velocity in this range is generally reduced, reaching the minimum around 0.3 µm (Petroff et al., 2008a; Litschke and Kuttler, 2008). Several dry deposition models that capture this behaviour have been proposed (Slinn, 1982; Seinfeld and Pandis, 2006; Petroff et al., 2008b; Petroff and Zhang, 2010), mostly for

use in the large scale models. The proposed models differ in the processes included and in the exact parameterization of the processes.

In this paper we want to investigate the influence of the street canyon vegetation on the pollutant dispersion, taking the size-dependent effects into account. We assume that the particle size distribution of the pollutant at the source is known. Two approaches to the modelling of the particle size distribution can be used. First is a sectional approach, which consists of dividing the size range under investigation into a number of discrete bins and then solving a transport equation for every bin separately. The other option is a so called moment method, where one models the transport of the moments of the particle size distribution. Such approach is often used in the large scale models (e.g. Binkowski and Shankar, 1995), but less so in the microscale CFD models.

As the mathematical formulation of the moment equations is constraining the possible form of the terms in the equation, the usage of a dry deposition model in the moment method is not straightforward. In (Šíp and Beneš, 2016) we adapted the model by Petroff et al. (2008b) for use in the microscale moment method solver and showed that such approach is of comparable accuracy to the sectional model, while at the same time providing significant improvements in the computational performance.

Using this model, we investigate the influence of the dry deposition on the concentration levels in the street canyon. For the fixed geometry, the flow under the varying inlet flow angle is examined, and the effect of the vegetation on the ultrafine, accumulation and coarse mode particles is assessed.

## 2 NUMERICAL MODEL

### 2.1 Fluid flow

The flow field was calculated using a 3D finite volume solver implemented using the OpenFOAM framework (Greenshields, 2015). A customized solver was developed on the basis of the *simpleFoam* solver, adding the proper boundary conditions for atmospheric boundary layer flows and a vegetation model. The solver is based on the Reynolds-averaged Navier-Stokes equations of the incompressible flow,

$$\nabla \cdot \boldsymbol{u} = 0, \tag{1}$$

$$\frac{\partial \boldsymbol{u}}{\partial t} + (\boldsymbol{u} \cdot \nabla)\boldsymbol{u} + \nabla p = \nabla \cdot (\nu_E \nabla \boldsymbol{u}), \tag{2}$$

where $\boldsymbol{u}$ is velocity, $p$ is pressure, and $\nu_E$ is effective viscosity. This physical model is valid for neutrally stratified flows at small scales, and unless thermal or stratification effects are expected, it is suitable for use in the urban CFD models. The solver uses the SIMPLE algorithm (Patankar and Spalding, 1972) to obtain a steady state solution of the system. The flow equations are complemented by the standard k-$\epsilon$ turbulence model.

We model the vegetation as horizontally homogenous, described by its vertical *leaf area density* (LAD) profile - the foliage surface area per unit volume - and its drag coefficient, $C_d$. The effect of the vegetation is modelled by adding the following source and sink terms to the moment and turbulence equations:

$$\left(\frac{\partial \boldsymbol{u}}{\partial t}\right)_{\text{veg}} = -C_d \text{LAD} |\boldsymbol{u}| \boldsymbol{u}, \tag{3}$$

$$\left(\frac{\partial k}{\partial t}\right)_{\text{veg}} = S_k = C_d \text{LAD} (\beta_p |\boldsymbol{u}|^3 - \beta_d |\boldsymbol{u}| k), \tag{4}$$

$$\left(\frac{\partial \epsilon}{\partial t}\right)_{\text{veg}} = C_{\epsilon_4} \frac{\epsilon}{k} S_k, \tag{5}$$

with the constants $\beta_p = 1.0$, $\beta_d = 5.1$ and $C_{\epsilon_4} = 0.9$ (Katul et al., 2004).

The choice of the proper boundary conditions for ABL flows is a well-discussed problem in the research community (Richards and Hoxey, 1993; Hargreaves and Wright, 2007; Parente et al., 2011; Balogh et al., 2012). In our model, we use the inlet profiles and wall functions given by Richards and Hoxey (1993). That is, at the inlet the wind profile is given by $u(z) = u^*/\kappa \log\left((z + z_0)/z_0\right)$, turbulence kinetic energy is specified as $k(z) = {u^*}^2/\sqrt{C_\mu}$, and turbulent dissipation rate as $\epsilon(z) = {u^*}^3/(\kappa z)$, where $\kappa = 0.41$ is the von Kármán constant, $z_0$ is the surface roughness length, and $u^*$ is the friction velocity. Prescribed values for the velocity, turbulent dissipation rate and turbulent production at the first cell above the ground are specified using the formulation given by Parente et al. (2011), which reduces the near-ground artificial peak of the turbulent kinetic energy produced by the original formulation.

The inlet wind profile in the original experiment is described by the power law, $u(z) = u_{\mathrm{ref}}(z/z_{\mathrm{ref}})^{\alpha}$ with $z_{\mathrm{ref}} = H$, $u_{\mathrm{ref}} = 4.39\,\mathrm{m\,s^{-1}}$ and $\alpha = 0.3$. To replace this power law form with the log profile, friction velocity $u^*$ and surface roughness length $z_0$ were chosen to minimize the quadratic error of the both formulations on the interval [0; 2H], resulting in $u^* = 0.50\,\mathrm{m\,s^{-1}}$ and $z_0 = 0.39\,\mathrm{m}$.

### 2.2 Pollutant dispersion

The pollutant dispersion is modelled using the approach described in (Šíp and Beneš, 2016). The method is based on the ideas of the moment method (Whitby and McMurry, 1997). The basic assumption is that the particle size distribution is composed of several modes, and that each of them can be represented as a lognormal distribution. For each mode a set of three partial differential equations can be written, describing the behaviour of three moments $M_k = \int_0^\infty d_p^k n(d_p)\mathrm{d}d_p$ of the particle size distribution $n(d_p)$. These equations are derived from the transport equation of the particle number concentration,

$$\frac{\partial n(d_p)}{\partial t} = -\underbrace{\nabla\cdot\boldsymbol{u}n(d_p)}_{\text{Convection}} + \underbrace{\nabla\cdot\frac{\nu_E}{\mathrm{Sc}}\nabla n(d_p)}_{\text{Diffusion}} - \underbrace{\nabla\cdot\boldsymbol{g}\frac{d_p^2\rho_p}{18\mu}n(d_p)}_{\text{Gravitational settling}} - \underbrace{\mathrm{LAD}u_d(d_p)n(d_p)}_{\text{Deposition}}, \tag{6}$$

where Sc is the turbulent Schmidt number, $\boldsymbol{g}$ is the gravitational acceleration, $\rho_p$ is the density of the particle, $\mu$ is the dynamic viscosity of the air, LAD stands for the leaf area density of the vegetation, and $u_d$ is the dry deposition velocity. Other processes besides deposition and gravitational settling, such as coagulation, condensation or nucleation, are not considered here.

After multiplying Eq. (6) by $d_p^{k_i}$ and integrating over all diameters $d_p$, we obtain the equation for $k_i$-th moment,

$$\frac{\partial M_{k_i}}{\partial t} = -\underbrace{\nabla\cdot\boldsymbol{u}M_{k_i}}_{\text{Convection}} + \underbrace{\nabla\cdot\frac{\nu_E}{\mathrm{Sc}}\nabla M_{k_i}}_{\text{Diffusion}} - \underbrace{\nabla\cdot\boldsymbol{g}\frac{\rho_p}{18\mu}M_{k_i+2}}_{\text{Gravitational settling}} - \underbrace{\mathrm{LAD}\int_0^\infty d_p^k u_d(d_p)n(d_p)\mathrm{d}d_p}_{\text{Deposition}}, \quad i = 0,1,2. \tag{7}$$

The evaluation of the integral in Eq. (7) representing the deposition poses a problem for arbitrary form of the deposition velocity $u_d$. In (Šíp and Beneš, 2016) we adapted the size-resolved dry deposition model from (Petroff et al., 2008b) for use in the moment method. The process can be summarized as follows:

1. We start with the original model, which expresses the deposition velocity as a sum of deposition velocities representing the relevant physical processes, $u_d(d_p) = \sum_P u_P(d_p)$, where the processes $P$ are Brownian diffusion, interception, inertial and turbulent impaction, and sedimentation.

2. To allow the analytical evaluation of the integral in Eq. (7), the deposition velocities of all processes $u_P$ are expressed in a power law form of the particle diameter $d_p$. This is achieved either by a simplification of the original model or by a least-square fitting of a power law function to the original formula.

3. Finally, with the approximated deposition velocity the integral in Eq. (7) can be analytically evaluated. The dependence on the powers of the particle diameter $d_p$ is replaced by the dependence on the moments of higher orders. These can in turn be expressed using the three moments we solve for using the known relations of the lognormal distribution, so the deposition term can be written as

$$\left.\frac{\partial M_{k_i}}{\partial t}\right|_{\text{Deposition}} = F_i(M_{k_0}, M_{k_1}, M_{k_2}). \tag{8}$$

In our model, we work with the zeroth moment $M_0$, equal to the total number concentration, the second moment $M_2$, proportional to the surface area concentration, and the third moment $M_3$, proportional to the volume and mass concentration. The gravitational settling term and the deposition term introduce the coupling between the equations. After solving these three equations for every mode, parameters of the lognormal distributions corresponding to all modes can be reconstructed, giving us the shape of the particle size distribution everywhere in the modelled domain.

The original model and the adapted moment method model are formulated for the trees with needle-like leaves. For the broadleaves used in this study, one can use the same principles outlined in (Šíp and Beneš, 2016) to adapt the broadleaf model proposed in (Petroff et al., 2009). Deposition velocity obtained by the model and its dependence on the particle diameter is shown on Fig. 1.

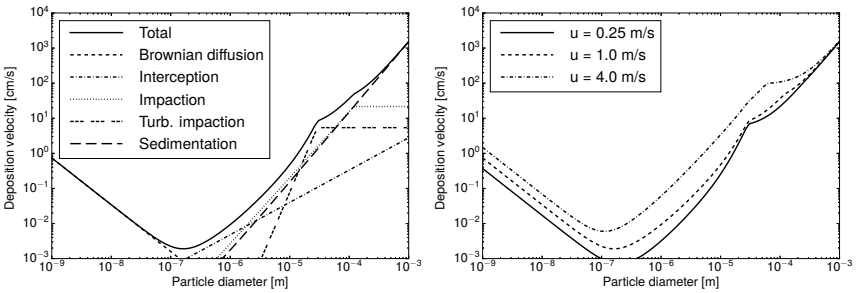


Figure 1: (Left) Deposition velocity according to the used model for the wind velocity $u = 1\,\mathrm{m\,s^{-1}}$ and the contributions of all processes. (Right) Dependence of the deposition velocity on the wind velocity. For both plots, following parameters are used: particle density $\rho_p = 1500\,\mathrm{kg\,m^{-3}}$, local friction velocity $u_f = 0.3\,\mathrm{m\,s^{-1}}$, leaf diameter $d_e = 0.03\,\mathrm{m}$.

### 2.3 Numerical implementation

The flow solver and the moment method solver are implemented in the OpenFOAM framework. The convective terms in the velocity equation (2), in the moment equations (7), and in the turbulence equations are dicretized using the second order upwind scheme. The second order scheme based on the Gauss theorem is used for the diffusive terms. We consider the iterative steady state solvers converged when the residuals drop below the threshold $10^{-6}$.

## 3 CASE SETTINGS

The pollutant dispersion in the street canyon was extensively studied by Gromke et al. through a series of wind tunnel experiments and CFD simulations (Gromke and Ruck, 2007; Gromke et al., 2008; Buccolieri et al., 2009; Gromke and Ruck, 2009; Buccolieri et al., 2011; Gromke and Ruck, 2012). The results were made available through an online database (CODASC, 2008). In this study we replicate one of the studied street canyon configuration, where the width of the street $W$ is equal to the height of the buildings $H$, i.e. $W/H = 1$. A sketch of the geometry is on Fig. 2.

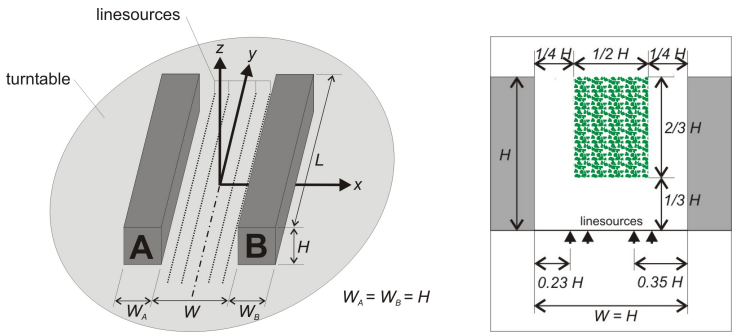


Figure 2: A sketch of the situation. (Left) 3D view of the experiment configuration without the trees. (Right) Side view of the street with the trees. Images reproduced from (CODASC, 2008). In the numerical experiments presented in the paper, $L = 10W$ and $W_A = W_B = W = H = 18\mathrm{m}$.

The computational mesh is created using the *snappyHexMesh* generator. The domain extends $6L$ upstream, downstream and to the sides from the street canyon. The mesh is progressively refined near the street canyon, and the canyon itself is composed of 26 cells across the street, 260 cells in the direction parallel to the street, and 42 cells in the vertical direction. In total, approximately 2.6 millions cells are used in the whole domain. Computations on a finer mesh were performed to show that a further refinement does not change the solution significantly.

Configurations without and with trees present were simulated. When trees are present, the drag coefficient $C_d$ is set to 0.3 as a value representing typical vegetation (Katul et al., 2004). The LAD profile is set to constant $1.77\,\mathrm{m^2\,m^{-3}}$, so that the product $\lambda = C_d\mathrm{LAD}$ is a full-scale equivalent of the pressure loss coefficient $\lambda^{wt} = 80\,\mathrm{m^{-1}}$ reported for the wind tunnel measurements (Gromke and Ruck, 2012).

| | Without trees | | | | | With trees | | | | |
|---|---|---|---|---|---|---|---|---|---|---|
| | Max WT | Max CFD | NMSE | FB | FAC2 | Max WT | Max CFD | NMSE | FB | FAC2 |
| 90°, wall A | 42.57 | 66.60 | 0.27 | -0.03 | 0.82 | 59.22 | 87.62 | 0.75 | -0.05 | 0.47 |
| 90°, wall B | 11.81 | 21.00 | 0.26 | -0.21 | 0.95 | 6.13 | 31.02 | 2.96 | -0.63 | 0.31 |
| 45°, wall A | 46.48 | 43.52 | 0.22 | 0.36 | 0.73 | 79.19 | 158.24 | 1.03 | 0.03 | 0.21 |
| 45°, wall B | 10.76 | 6.77 | 0.40 | 0.45 | 0.71 | 7.47 | 56.84 | 10.68 | -1.42 | 0.15 |
| 0°, wall A and B | 32.00 | 28.44 | 0.11 | 0.02 | 0.79 | 44.76 | 56.69 | 0.15 | -0.19 | 0.71 |

Table 1: Maximal values of non-dimensional particle number concentration on street canyon walls and three evaluation criteria following (Hanna et al., 2004). Abbreviations: Max WT = Maximal value in wind tunnel measurements, Max CFD = Maximal value in CFD simulation, NMSE = Normalized mean square error, FB = fractional bias, FAC2 = factor of two of observations. Measurement values taken from (CODASC, 2008).

The pollutant dispersion under three wind conditions was modelled: with wind parallel to the street (angle 0°), under angle 45° relative to the street and perpendicular to the street (angle 90°). Same mesh was used for all simulations. For the flow under the angles 0° and 90°, the upstream boundary plane is set as inlet, the downstream plane as outlet, and the lateral planes are set as symmetry walls. For the flow under 45° (i.e. diagonal) flow, two upstream planes are set as inlet and two downstream planes are set as outlet. In all cases, the inlet wind velocity at the height of the top of the buildings was set to $u_{\mathrm{ref}} = 4.673\,\mathrm{m\,s^{-1}}$. Following (Vranckx et al., 2015), the Schmidt number is set to 0.3.

The behaviour of three modes of particle size distribution was examined. The three modes, described as lognormal distributions, were the ultrafine mode (geometric mean size $d_{gn} = 0.014\,\mu\mathrm{m}$, geometric standard deviation $\sigma_g = 1.81$), the accumulation mode ($d_{gn} = 0.054\,\mu\mathrm{m}$, $\sigma_g = 2.16$), and the coarse mode ($d_{gn} = 0.86\,\mu\mathrm{m}$, $\sigma_g = 2.21$), typical for urban environment (Hinds, 1999). Four line sources of the pollutant were placed inside the street canyon, all at the height 1 m above the ground and at a distance from the buildings as depicted on Fig. 2, right panel.

## 4 RESULTS

### 4.1 Comparison with the wind tunnel data

The obtained results were compared to the available wind tunnel data (CODASC, 2008). Only partial comparison is presented here. The results for the ultrafine mode, virtually unaffected by the gravitational settling, and without the deposition taken into account, were taken as an analogue to the wind tunnel measurements. Table 1 shows the maximal values of the non-dimensional number concentrations,

$$c_n^+ = \frac{c_n u_{\mathrm{ref}} H}{Q_n/l}, \tag{9}$$

where $c_n$ is the number concentration and $Q_n/l$ is the particle number source intensity per unit length. Furthermore, three criteria evaluating the fit between the CFD and the wind tunnel results following (Hanna et al., 2004) are presented. The values are shown for the leeward wall A and windward wall B.

Hanna et al. (2004) offered following acceptance criteria: normalized mean square error NMSE < 4, fractional bias FB $\in$ [-0.3, 0.3], and the fraction of predictions within a factor of two of observations FAC > 0.5. Generally, good agreement following these criteria was observed for the cases without the vegetation and for the angles 90° and 0°, even if the maxima for the perpendicular flow are increased.

When the vegetation is present the agreement is good for the flow parallel to the street, yet significantly worse for the other cases. The most notable difference is for the flow under 45° angle. Major overprediction is caused by a backflow at the end of the street canyon, resulting in the rise of the concentration close to the end of the canyon (see Fig. 3).

Nevertheless, even if the flow pattern differs from the measurements, the results can still be useful in providing some answers about the impact of the dry deposition on the concentration, discussed in the next section.

### 4.2 Effect of the dry deposition

Table 2 shows the amount of the pollutant deposited on the vegetation as a percentage of the amount of the pollutant inserted into the domain as the vehicular emissions. The percentage for the particle count

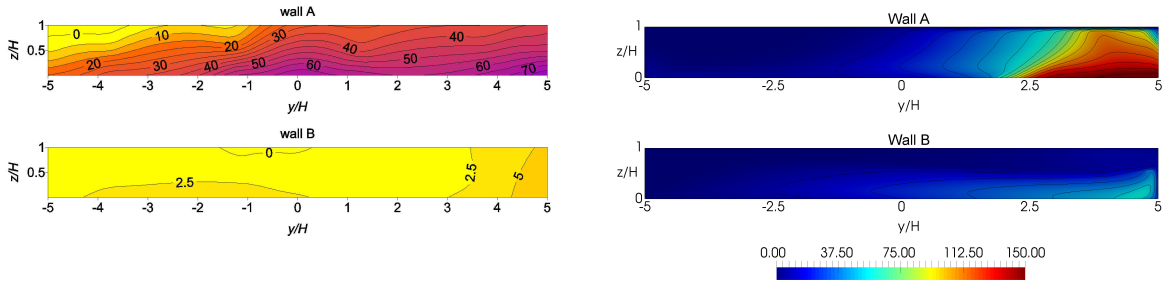


Figure 3: Non-dimensional concentration at the street canyon walls for the flow under the angle 45° relative to the canyon and with the trees. Shown are the measurement data obtained from (CODASC, 2008) (left) and CFD results (right). A significant concentration increase due to the backflow is visible at both walls near the end of the street canyon for the CFD results.

| | Ultrafine | | Accumulation | | Coarse | |
|---|---|---|---|---|---|---|
| | Particle count | Mass | Particle count | Mass | Particle count | Mass |
| 90° | 0.60% | 0.15% | 0.13% | 0.07% | 0.29% | 6.29% |
| 45° | 0.53% | 0.13% | 0.12% | 0.06% | 0.26% | 5.20% |
| 0° | 0.32% | 0.08% | 0.07% | 0.04% | 0.15% | 2.98% |

Table 2: Percentage of the amount of pollutant deposited on the vegetation compared to the amount of the pollutant inserted in the domain.

as well as for the mass deposited is presented for all three modes.

The accumulation mode is affected by the deposition only negligibly. The peak of the number distribution and the mass distribution of the mode is close to the minimum of the deposition velocity curve (see Fig. 1) and as a result, less than 0.15% of the exhausted particles and of their mass is deposited on the vegetation. The ultrafine and the coarse modes are affected more, reflecting the higher deposition velocity due to the Brownian diffusion for the smaller particles and due to the impaction, interception and gravitational settling for the larger particles. Still, the number of deposited particles in the ultrafine mode is below 1% in all cases. Only when looking at the deposited mass in the coarse mode the effect of the dry deposition becomes notable.

Tables 3 and 4 show the maximal values of the non-dimensional number concentration and mass concentration respectively at the street canyon walls. All simulated cases are included in the tables. Again, for the accumulation mode the effects of the dry deposition process are almost nonexistent. Also the difference for the ultrafine mode is below 1% in the number concentration and below 0.25% in the mass concentration.

The effect of the dry deposition on the coarse mode is more pronounced, especially looking at the mass concentration. In most cases, the difference in the maximal values at the walls is around 2%. Such effect is however insignificant compared to the concentration increase that is caused by the other consequence of the street canyon vegetation, which is the restricted mixing between the air at the pedestrian level and the air above the buildings.

The only configuration where we observe a significant role of the dry deposition is the flow perpendic-

| | Ultrafine | | | | Accumulation | | | | Coarse | | | |
|---|---|---|---|---|---|---|---|---|---|---|---|---|
| | NT | TND | TD | Diff | NT | TND | TD | Diff | NT | TND | TD | Diff |
| 90°, wall A | 66.60 | 87.62 | 87.49 | 0.14% | 66.60 | 87.62 | 87.59 | 0.03% | 66.61 | 87.63 | 87.57 | 0.07% |
| 90°, wall B | 21.00 | 31.02 | 30.72 | 0.98% | 21.00 | 31.02 | 30.95 | 0.21% | 20.99 | 31.01 | 30.87 | 0.46% |
| 45°, wall A | 43.52 | 158.25 | 158.10 | 0.09% | 43.52 | 158.25 | 158.22 | 0.02% | 43.52 | 158.14 | 158.07 | 0.04% |
| 45°, wall B | 6.77 | 56.84 | 56.80 | 0.07% | 6.77 | 56.84 | 56.83 | 0.01% | 6.77 | 56.80 | 56.78 | 0.04% |
| 0°, wall A and B | 28.44 | 56.69 | 56.64 | 0.08% | 28.44 | 56.69 | 56.68 | 0.02% | 28.43 | 56.66 | 56.63 | 0.04% |

Table 3: Maximal values of the non-dimensional particle number concentration at the walls. Abbreviations: NT = no trees, TND = trees, no deposition, TD = trees with deposition, Diff = (TND - TD)/TD = Relative difference between TND and TD.

| | Ultrafine | | | | Accumulation | | | | Coarse | | | |
|---|---|---|---|---|---|---|---|---|---|---|---|---|
| | NT | TND | TD | Diff | NT | TND | TD | Diff | NT | TND | TD | Diff |
| 90°, wall A | 66.60 | 87.62 | 87.58 | 0.04% | 66.60 | 87.62 | 87.60 | 0.02% | 66.53 | 87.81 | 86.29 | 1.76% |
| 90°, wall B | 21.00 | 31.02 | 30.94 | 0.25% | 21.00 | 31.02 | 30.98 | 0.11% | 20.67 | 30.60 | 27.25 | 12.29% |
| 45°, wall A | 43.52 | 158.25 | 158.21 | 0.02% | 43.52 | 158.24 | 158.22 | 0.01% | 43.46 | 153.23 | 151.32 | 1.27% |
| 45°, wall B | 6.77 | 56.84 | 56.83 | 0.02% | 6.77 | 56.83 | 56.83 | 0.01% | 6.65 | 54.99 | 54.49 | 0.91% |
| 0°, wall A and B | 28.44 | 56.69 | 56.68 | 0.02% | 28.44 | 56.68 | 56.68 | 0.01% | 27.78 | 55.16 | 54.58 | 1.07% |

Table 4: Same as Tab. 3, but for non-dimensional mass concentration.

ular to the street canyon. In that case, the maximum in the mass concentration at the wall B is reduced by approximately 12%. This is caused by the fact that the polluted air is filtered before it reaches the wall B. Unlike in other cases, the pollutant released at the middle of the street circulates around the street canyon: first to the wall A, then through the canopy at the top of the canyon and then to the wall B. As the air flows through the tree crowns, the pollutant is partially removed by the dry deposition, so the air reaches the wall B with the pollutant concentrations reduced. However, the filtering happens only after the polluted air flows around the wall A, so the wall A is left unprotected.

## 5 CONCLUSIONS

Using the moment method, we investigated the effect of the vegetation inside the street canyons. The trees were shown to block the circulation and as a result to increase the pollutant concentrations at the street level. Such observation is in line with the previous research (Gromke and Ruck, 2012; Janhäll, 2015).

The impact of the dry deposition is shown to vary for different modes. The accumulation mode with the geometric mean size 0.054 µm is virtually unaffected by the vegetation. The concentration difference caused by the deposition locally rises up to 1% for the ultrafine mode. That is however still negligible compared to the effects caused by the altered flow field. For the coarse mode particles, around 5% of the mass inserted into the domain at the street level is deposited on the vegetation, and the mass concentration is locally reduced by more than 10% in some cases.

The effect on the pedestrian level is most significant when the pollutant laden air flows through the canopy so that the air is filtered. If this does not apply, researchers can be justified in not including the dry deposition process in the microscale model.

Background concentration, present in the urban environment, was not considered in the model. If it was, the effect of the street canyon trees on the pollution levels would be reduced. That is because the ambient concentration, less affected by the flow patterns, would contribute more to the concentration at the street level, leaving the local sources with smaller influence. Also the possibility that the absorbing capacity of the leaves can change as more material is deposited was not considered here.

## ACKNOWLEDGEMENTS

This work was supported by the grant SGS16/206/OHK2/3T/12 of the Czech Technical University in Prague.

## REFERENCES

Balogh, M., Parente, A., and Benocci, C., 2012. RANS simulation of ABL flow over complex terrains applying an enhanced k-$\epsilon$ model and wall function formulation: Implementation and comparison for fluent and OpenFOAM. J. Wind Eng. Ind. Aerodyn., 104-106:360–368.

Binkowski, F. and Shankar, U., 1995. The regional particulate matter model: 1. model description and preliminary results. J. Geophys. Res., 100(D12):26191–26209.

Buccolieri, R., Gromke, C., Sabatino, S. D., and Ruck, B., 2009. Aerodynamic effects of trees on pollutant concentration in street canyons. Sci. Total Environ., 407(19):5247–5256.

Buccolieri, R., Salim, S. M., Leo, L. S., Sabatino, S. D., Chan, A., Ielpo, P., de Gennaro, G., and Gromke, C., 2011. Analysis of local scale tree–atmosphere interaction on pollutant concentration in idealized street canyons and application to a real urban junction. Atmos. Environ., 45(9):1702–1713.

CODASC 2008. CODASC data base. Laboratory of Building- and Environmental Aerodynamics, Karlsruhe Institute of Technology KIT. http://www.ifh.uni-karlsruhe.de/science/aerodyn/CODASC.htm. [Online; accessed 21-March-2016].

Greenshields, C. J. 2015. OpenFOAM - The Open Source CFD Toolbox - User's Guide. Version 3.0.0. CFD Direct Ltd.

Gromke, C., Buccolieri, R., Sabatino, S. D., and Ruck, B., 2008. Dispersion study in a street canyon with tree planting by means of wind tunnel and numerical investigations – evaluation of CFD data with experimental data. Atmos. Environ., 42(37):8640–8650.

Gromke, C. and Ruck, B., 2007. Influence of trees on the dispersion of pollutants in an urban street canyon—experimental investigation of the flow and concentration field. Atmos. Environ., 41(16):3287–3302.

Gromke, C. and Ruck, B., 2009. On the impact of trees on dispersion processes of traffic emissions in street canyons. Boundary-Layer Meteorol., 131(1):19–34.

Gromke, C. and Ruck, B., 2012. Pollutant concentrations in street canyons of different aspect ratio with avenues of trees for various wind directions. Boundary-Layer Meteorol., 144(1):41–64.

Hanna, S. R., Hansen, O. R., and Dharmavaram, S., 2004. Flacs cfd air quality model performance evaluation with kit fox, must, prairie grass, and emu observations. Atmos. Environ., 38(28):4675–4687.

Hargreaves, D. and Wright, N., 2007. On the use of the k– model in commercial CFD software to model the neutral atmospheric boundary layer. J. Wind Eng. Ind. Aerodyn., 95(5):355–369.

Hinds, W., 1999. Aerosol technology: Properties, Behavior, and Measurement of Airborne Particles. Wiley, 2nd edition.

Janhäll, S., 2015. Review on urban vegetation and particle air pollution - deposition and dispersion. Atmos. Environ., 105:130–137.

Katul, G., Mahrt, L., Poggi, D., and Sanz, C., 2004. One- and two-equation models for canopy turbulence. Bound. Layer Meteor., 113:81–109.

Litschke, T. and Kuttler, W., 2008. On the reduction of urban particle concentration by vegetation - a review. Meteorol. Z., 17:229–240.

Parente, A., Gorlé, C., van Beeck, J., and Benocci, C., 2011. Improved k–$\epsilon$ model and wall function formulation for the RANS simulation of ABL flows. J. Wind Eng. Ind. Aerodyn., 99(4):267–278.

Patankar, S. V. and Spalding, D. B., 1972. A calculation procedure for heat, mass and momentum transfer in three-dimensional parabolic flows. Int. J. Heat Mass Transfer, 15(10):1787–1806.

Petroff, A., Mailliat, A., Amielh, M., and Anselmet, F., 2008a. Aerosol dry deposition on vegetative canopies. Part I: Review of present knowledge. Atmos. Environ., 42:3625–3653.

Petroff, A., Mailliat, A., Amielh, M., and Anselmet, F., 2008b. Aerosol dry deposition on vegetative canopies. Part II: A new modelling approach and applications. Atmos. Environ., 42(16):3654–3683.

Petroff, A. and Zhang, L., 2010. Development and validation of a size-resolved particle dry deposition scheme for application in aerosol transport models. Geoci. Model Dev., 3:753–769.

Petroff, A., Zhang, L., Pryor, S., and Belot, Y., 2009. An extended dry deposition model for aerosols onto broadleaf canopies. J. Aerosol Sci., 40(3):218–240.

Richards, P. and Hoxey, R., 1993. Appropriate boundary conditions for computational wind engineering models using the k-$\epsilon$ turbulence model. J. Wind Eng. Ind. Aerodyn., 46 & 47:145–153.

Seinfeld, J. and Pandis, S., 2006. Atmospheric Chemistry and Physics: From Air Pollution to Climate Change. A Wiley-Interscience publication. Wiley, 2nd edition.

Slinn, W., 1982. Predictions for particle deposition to vegetative canopies. Atmos. Environ., 16(7):1785–1794.

Vranckx, S., Vos, P., Maiheu, B., and Janssen, S., 2015. Impact of trees on pollutant dispersion in street canyons: A numerical study of the annual average effects in Antwerp, Belgium. Sci. Total Environ., 532:474–483.

Whitby, E. and McMurry, P., 1997. Modal aerosol dynamics modeling. Aerosol Sci. Technol., 27(6):673–688.

Šíp, V. and Beneš, L., 2016. Dry deposition model for a microscale aerosol dispersion solver based on the moment method. arXiv e-print. http://arxiv.org/abs/1605.03397.